KECK Geology Consortium
Learning Science Through Research
Published by Keck Geology Consortium
Short Contributions
29th Annual Symposium Volume
23rd April, 2016
ISBN: 1528-7491

DEFORMATION MECHANISMS AND QUARTZ CRYSTALLOGRAPHIC PREFERRED ORIENTATIONS AT VARYING STRUCTURAL LEVELS IN A CRUSTAL-SCALE EXTENSIONAL MYLONITIC SHEAR ZONE, EAST HUMBOLDT RANGE, CLOVER HILL, AND WOOD HILLS, ELKO COUNTY NEVADA

LINDSEY PLUMMER, Amherst College
JEFFREY M. RAHL, Washington and Lee University
ALLEN J. MCGREW, The University of Dayton
PETER CROWLEY, Amherst College

ABSTRACT

The Ruby Mountains-East Humboldt Range-Wood Hills metamorphic core complex in northeastern Nevada offers an unusual opportunity to trace the evolution and development of a 1km thick crustal-scale extensional mylonitic shear zone. An east-to-west transect from the Wood Hills through Clover Hill to the East Humboldt Range exposes progressively deeper structural levels of the mylonitic lower-plate of the Oligocene to earliest Miocene Ruby Mountain detachment fault.

Quartz deformation mechanisms have been inferred from the crystallographic-preferred orientations (CPOs) determined by electron backscatter diffraction (EBSD) for eight quartz-rich samples mylonitized within the shear zone. All of the samples have strong quartz crystallographic preferred orientations consistent with previously published reports. C-axis maxima range from 5-6 times uniform distribution in granitoid samples to 19-24 times uniform distribution in mylonitic quartzite. Though somewhat weaker, quartz CPOs from the mylonitic orthogneisses are consistent with those from nearby quartzites; they also serve to bracket the age of deformation between the early Oligocene age of the granitoids and earliest Miocene $^{40}Ar/^{39}Ar$ biotite cooling ages. The nature of the quartz CPOs changes systematically down the dip of the Ruby Mountain detachment. The structurally highest Wood Hills mylonites have quartz CPOs with c-axes distributed about an asymmetric girdle. This CPO is interpreted to be the result of quartz deformation with a significant contribution by basal <a> slip. Mylonites from structurally deeper Clover Hill outcrops have a quartz CPO with quartz c-axes forming an asymmetric girdle centered on Y, a fabric interpreted to have formed by a combination of rhomb <a> and prism <a> slip. Mylonites from the structurally deepest outcrops from the East Humboldt Range have quartz CPOs characterized by c-axis maxima parallel to Y, suggesting deformation dominated by prism <a> slip. This transition from basal <a> to rhomb <a> to prism <a> slip results from deformation at progressively higher temperatures towards the structurally deeper parts of the shear zone.

INTRODUCTION TO GEOLOGIC SETTING

This study examined a transect across the Ruby Mountains (RM)-East Humboldt Range (EHR) metamorphic core complex from mid-crustal exposures in the Wood Hills (WH) to deeper crustal levels in Clover Hill (CH) and even deeper levels in

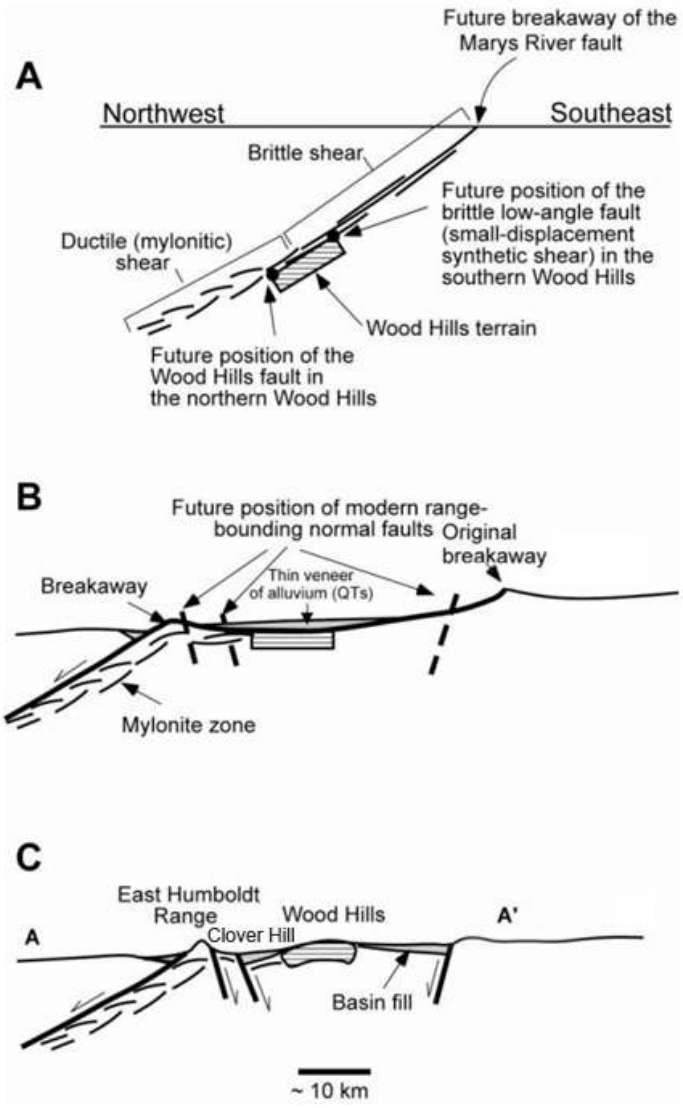

Figure 1. Schematic cross sections illustrating exhumation of the metamorphic rocks in the Wood Hills, Clover Hill and East Humboldt Range from Camilleri 2010. Note the progressively increasing structural depth of the mylonites toward the west.

the northern East Humboldt Range (EHR) (Fig. 1). K-Ar and $^{40}Ar/^{39}Ar$ mica cooling age "chrontours" show the WNW-progression of extensional unroofing facilitated by this shear zone (See Fig. 2, Rahl and McGrew, this volume).

The EHR-CH-WH metamorphic core complex was unroofed by normal-sense, top-WNW movement along the Ruby Mountain detachment fault. Proceeding westward from the WH to the EHR, progressively deeper levels of the RM-EHR detachment fault are exposed. Younger range-bounding high-angle normal faults offset the shear zone. Figure 1 (Camilleri 2010) illustrates the

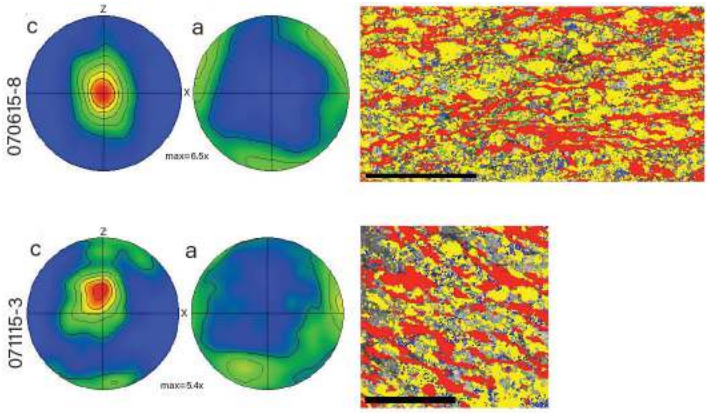

Figure 2. Pole figures (c- and a-axes) and texture maps of East Humboldt samples 070615-8 and 071115-3. In maps, scale=5mm, red=quartz, yellow=plagioclase, blue=orthoclase, green=muscovite.

evolution of the WNW-directed extensional shear zone from its initiation through its eventual segmentation by younger antithetic normal fault systems. Exposures of the shear zone have not been found in the easternmost part of the metamorphic core complex in the Pequop Mountains.

One sample, an Oligocene mylonitic biotite monzogranitic orthogneiss from the EHR, was located more specifically in the middle of a late-stage normal-sense shear that provides a small-scale analog to the crustal-scale shear zone. The exposure shows a down to the WNW normal-sense shear zone (>1m thick) that offsets ~30 Ma monzogranitic orthogneiss by ~10m.

METHODS

Field Methods

Samples for this study came from the Wood Hills, Clover Hill, and the Angel Lake cirque in the East Humboldts. All samples were oriented on foliation and lineation in the field. Four samples are from the Angel Lake region of the EHR, the structurally deepest of our three localities: two mylonitic biotite monzogranitic orthogneisses, one Cambrian quartzite from the Prospect Mountain unit, and one intensely recrystallized quartz vein. Two samples are from Clover Hill representing intermediate structural levels: two mylonitic quartzites from neighboring outcrops, but one with an interlayer of leucogranitic gneiss. The two samples from Wood Hills are both

from the Eureka Quartzite unit. In the Wood Hills, the intense shattering of the quartzite and the wide variety of orientations of graphite streaks rendered the recognition of lineation and foliation nearly indecipherable. Based on optical inspection, sample 070915-1 from the Wood Hills was almost certainly misoriented in the field. Interpretations of pole figures for this thin section will be presented with notes on its reinterpreted orientation.

Sample Preparation and Analytical Methods

Standard thin sections of each sample were cut perpendicular to foliation and parallel to lineation. Initially, samples were examined in hand sample and thin sections examined by optical microscopy for shear sense indicators, and where relevant, deformation mechanisms in quartz and feldspar. An electron backscatter diffraction and scanning electron microscope system (EBSD-SEM) was used to process each sample, some more successfully than others, resulting in a grain map and pole figures of quartz CPO trends of each thin section. Six samples, two from each locality, indexed well enough on the SEM to produce interpretable pole figures. These are discussed below.

RESULTS AND DISCUSSION

East Humboldt Range

Under the optical microscope, samples from the relatively deepest structural levels of the mylonitic zone exhibit strong fabrics and intensive dynamic recrystallization. The edges of ribbon grains are commonly consumed by very fine recrystallized grains and areas of subgrain polygonization, indicating recrystallization by progressive subgrain rotation (Stipp et al., 2002). Figure 2 shows texture maps and pole figures of the two samples that generated the most meaningful CPOs, 070615-8 and 071115-3. 071115-3, a mylonitic biotite monzogranitic orthogneiss, has an S-C fabric visible under magnification (Fig. 2) and in hand sample. Feldspar crystals between quartz grains appear to have acted as obstacles around which long quartz ribbon grains, oblique to foliation with an asymmetry indicating top-WNW normal-sense shear, flow.

Minerals such as muscovite which have also grown and recrystallized at high temperature appear to impede the rotation and growth of adjacent quartz grains. In 070615-8, another mylonitic biotite monzogranitic orthogneiss, these intergrowths dominate the fabric and appear not only to have impeded quartz reorientation, but also have guided the quartz into channels between other minerals that are typically aligned under pressure (Fig. 2). It is not clear whether this resulted in the same c-axis orientations that would have developed had quartz moved freely under the strain of the shear zone, but hand sample has sigma clasts and other shear-sense indicators yielding a consistent WNW shear sense.

Quartz pole figures show strong single <c> axis maxima that are parallel to Y with an <a> axis maximum that is oblique to X. This pattern is produced by prism <a> slip. In thin-sections of 070615-8 and 071115-3, pole figures of feldspar also show some preferred orientations (Fig. 3). Albite porphyroclasts from the EHR show evidence of both brittle and plastic deformation. Some porphyroclasts are cut by mica-filled fractures; other porphyroclasts have undulose and patchy extinction. Both albite

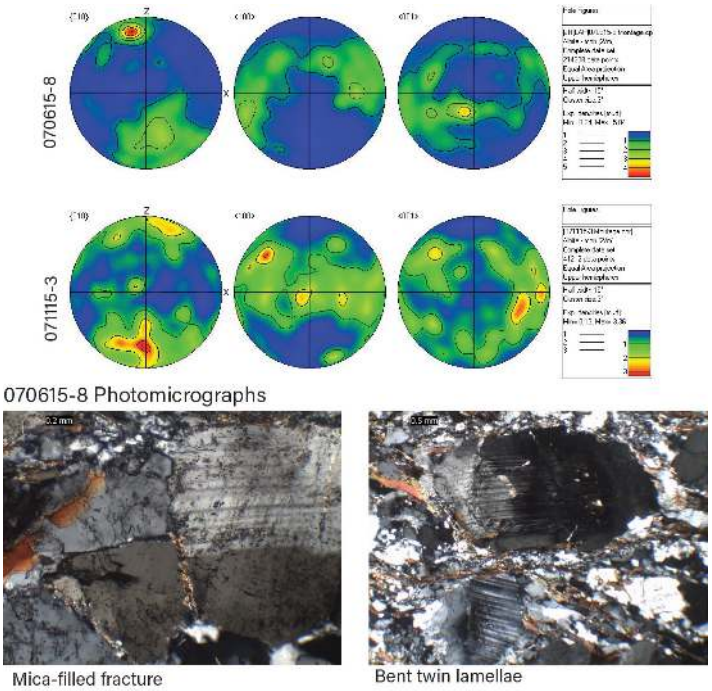

Figure 3. Feldspar pole figures and photomicrographs of EHR samples 070615-8 and 071115-3. Micrographs depict albite bent twin lamellae in 070615-8 and mica-filled fractures in 071115-8.

and pericline twins occur, and twin lamellae are both straight and gently curved. Albite has a weak to moderate crystallographic fabric with [010] slightly oblique to foliation suggesting a weak alignment of the composition plane of albite twins with foliation.

Clover Hill

Samples 071415-1a and b, both mylonitic quartzites, are amphibolite facies quartzites that exhibit both significant undulose and zoned extinction and deformation bands. Figure 4 includes pole figures and photomicrographs. Sample 071415-1b, which also includes leucogranite, has mica intergrowths resembling those of 070615-8. In hand sample, the mica highlights a strong lineation and a consistent WNW shear sense from mica fish relative to the plane of the fabric. Both samples have fabrics visible in hand sample and in thin section. Quartz pole figures in both samples (Fig. 4) show very strong c-axis concentrations near Y that spread into an asymmetrical girdle with a-axes oblique to X. This pattern could be produced by a combination of prism <a> and rhomb <a> slip. Photomicrographs (polarized light with a quartz plate) show serrate grain boundaries and a well-developed subgrain structure within coarse, intensely deformed quartz grains.

Wood Hills

Pole figures and photomicrographs of two Wood Hills quartzites are depicted in Figure 5. Quartz grains in 071315-1 are very serrated and exhibit little to no undulose extinction. Intricately interlocking grain boundaries suggesting recrystallization by bulge nucleation enveloped by a matrix of fine, polygonal neoblasts. 070915-1, the only other sample from the shallowest structural levels in the Wood Hills, has strong undulose extinction, only in the coarsest grains, which describes about 20% of its grains. These coarse (>1000 μm) ribbon grains with tabular subgrains and locally with transecting trains of fine, dynamically recrystallized neoblasts inclined to the long axis of the ribbons with a sense of asymmetry, suggesting sinistral shear sense parallel to the short sides of the photomicrograph.

The samples from the Wood Hills are problematic. Pole figures for 070915-1 show uninterpretable double- maxima that are oblique to sample axes. Photomicrographs (polarized light, quartz plate) show a grain shape fabric of fine-grained quartz at a high angle to “foliation” and “lineation”. Together these observations suggest that fabric elements were misidentified in the field. The pole figures to the bottom left of Figure 5 have been rotated to produce interpretable pole figures with asymmetrical <c> axis girdles with maxima that are oblique to Z and <a> axes oblique to X. This type of pattern is characteristic of basal <a> slip, commonly considered the lowest

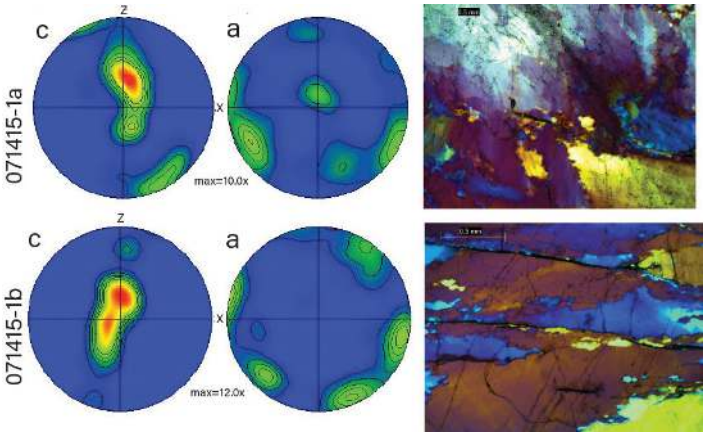

Figure 4. Pole figures (c- and a-axes) and photomicrographs of Clover Hill samples 071415-1a and 071415-1b. Micrographs show serrate grain boundaries and a well-developed sub-grain structure within large highly deformed quartz grains.

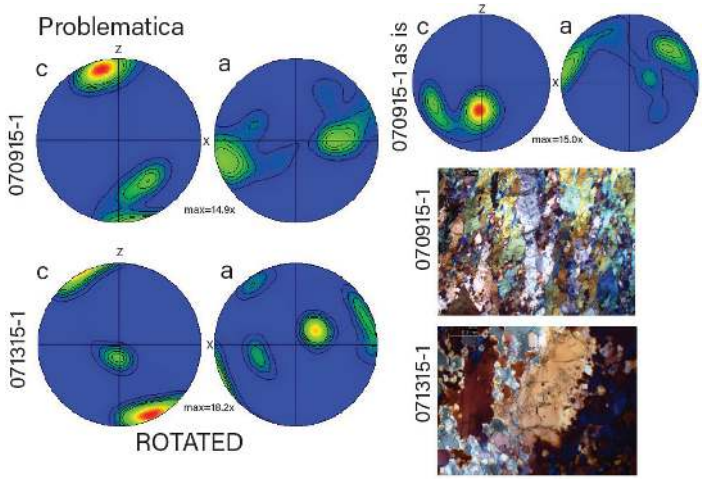

Figure 5. Pole figures (c- and a-axes) and photomicrographs of Wood Hills samples 070915-1 and 071315-1. Pole figures on top right are the initial, misoriented images from sample 070915-1, and figures on bottom left are reoriented in accordance with petrographic observations of foliation and lineation in thin section.

temperature deformation mechanism in quartz. Rotating the samples creates a WNW (071315-1) or WSW (070915-1) plunging "new X" or lineation direction. This is consistent with the inferred regional top to the WNW shearing direction.

CONCLUSIONS

Quartz grain and crystallographic preferred orientations change systematically across the EHR-CH-WH core complex. In the Wood Hills, quartz appears to deform by subgrain rotation via basal <a> slip. At Clover Hill, deformation by grain boundary migration takes over, and the active slip systems in quartz are the prism and rhomb <a> systems. In the East Humboldt Range, quartz deformation occurs predominantly by prism <a> slip.

Deformation temperature can also be estimated based on quartz slip systems and recrystallization mechanisms. Quartz deformation by subgrain rotation by basal <a> slip is estimated (Stipp et al. 2002) to occur at temperatures between 400° and 500°C, with the transition to deformation by grain boundary migration and prism <a> slip occurring above ~500°C. There is no evidence of prism <C> slip in the samples analyzed in this study, suggesting that the deformation temperatures were below ~600°C; however, working at deeper structural levels beneath the mylonitic zone, Chevalier (this volume) reports evidence of fast grain boundary migration recrystallization and large opening-angle c-axis fabrics consistent with higher temperature deformation. With the transition into the gneissic infrastructure beneath the mylonitic shear zone, large opening angle CPOs are observed increasingly with depth. Such CPOs are commonly interpreted as indicating paired basal <a> and prism <c> slip. Together, these microstructures and CPOs strongly suggest deformation conditions in excess of 600°C. That interpretation is also supported by observed growth of zircon rims as young as 28 Ma and by resetting of $^{40}Ar/^{39}Ar$ Hbl ages at elevations beneath ~9500 ft. in Angel Lake cirque.

The EHR-WH core complex was penetratively deformed by both Mesozoic compressional and Cenozoic extensional events. Samples 070615-8 and 071115-3 from the EHR are Oligocene granitic gneisses with quartz deformation mechanisms and CPOs that resemble those developed in Paleozoic quartzites. Quartz behaves similarly in both the quartzite and the granitic gneiss, with both quartz- and feldspar-rich samples, showing similar microstructures and Y-maximum quartz CPOs suggesting prism <a> slip. This indicates that quartz is the weak mineral, controlling deformation in both rock types.

These deformation mechanisms also indicate that strain occurred at temperatures well above the $^{40}Ar/^{39}Ar$ closure temperature of micas (~300°C); thus the cooling of these rocks through $^{40}Ar/^{39}Ar$ biotite closure temperature by 22 Ma brackets the age of mylonitic deformation in the EHR between the mid-Oligocene age of the orthogneiss and the early Miocene biotite cooling ages (McGrew and Snee, 1994). However, up-dip parts of the mylonitic zone would have been processed through the mylonitic zone earlier in the exhumation history, and thus age constraints at shallower structural levels indicate earlier cooling. The deformation age of the Clover Hill mylonites must predate $^{40}Ar/^{39}Ar$ biotite cooling ages of approximately 27.5 Ma (Dallmeyer et al., 1986; Gifford (2008). In the NW Wood Hills, mylonitization must predate a new U-Th/He zircon cooling age of 41.8 Ma (the nominal closure temperature for U-Th/He zircon is 180°-220°C) (Wolfe, this volume).

ACKNOWLEDGEMENTS

Thank you to my enthusiastic Keck advisors Allen McGrew and Jeffrey Rahl for your mentorship and an incredible experience in the field, and to my Keck teammates for their comradery. Thank you to Peter Crowley, my advisor at Amherst, for four years of geologic inspiration and sticking with me to the end, and to the rest of the Amherst College Geology Department faculty and staff. Thank you to the Keck Geology Consortium, ExxonMobil, and the National Science Foundation for their sponsorship.

REFERENCES

Camilleri, P., 2010, Geologic map of the Wood Hills, Elko County, Nevada: Nevada Bureau of Mines and Geology Map, no. 172.

Dallmeyer, R. D., A. W. Snoke, and E. H. McKee (1986), The Mesozoic-Cenozoic tectonothermal evolution of the Ruby

Mountains, East Humboldt Range, Nevada: A Cordilleran Metamorphic Core Complex, Tectonics, 5(6), 931–954, doi:10.1029/TC005i006p00931.

Gifford, J, 2008, Quantifying Eocene and Miocene extension in the Sevier hinterland in Northeastern Nevada: Masters Thesis to University of Florida.

McGrew, A. and Casey, M., 1998, Quartzite fabric transition in a Cordilleran metamorphic core complex: Fault-related Rocks: A photographic atlas, p. 484-489.

McGrew, A. and Snee, L., 1994, $^{40}Ar/^{39}Ar$ thermochronologic constraints on the tectonothermal evolution of the northern East Humboldt Range metamorphic core complex, Nevada: Tectonophysics, no. 238, p. 425-450.

McGrew, A.J., and Snoke, A.W., 2015, Geologic map of the Welcome quadrangle and an adjacent part of the Wells quadrangle, Elko County, Nevada: Nevada Bureau of Mines and Geology, Map 184, 1:24,000; inset 1:12,000; text 40 p.

Stipp, Michael and Kunze, Karsten, "Dynamic Recrystallization near the Brittle-Plastic Transition in Naturally and Experimentally Deformed Quartz Aggregates," Tectonophysics 448, no. 1-4. (2008)

Stipp, M., Stünitz, H., Heilbronner, R. and Schmid, S.M., "The eastern Tonale fault zone: a `natural laboratory' for crystal plastic deformation of quartz over a temperature range from 250 to 700 8C," Journal of Structural Geology 24. (2002)